Low Temperature Physics/Fizika Nizkikh Temperatur, 2012, v. 38, No. 10, pp. 1184–1190

Influence of magnetic anisotropy on hysteresis behavior in the two-spin model of a ferro/antiferromagnet bilayer with exchange bias

A.G. Grechnev, A.S. Kovalev, and M.L. Pankratova

B. Verkin Institute for Low Temperature Physics and Engineering of the National Academy of Sciences of Ukraine
47 Lenin Ave., Kharkov 61103, Ukraine
E-mail: pankratova_mari@mail.ru

Received May 21, 2012

The influence of magnetic anisotropy of ferromagnetic film on the phenomenon of exchange bias is studied. Hysteresis behavior in the two-spin model of a ferro/antiferromagnet (FM/AFM) bilayer with exchange bias has been investigated in detail. In this model a half-space of AFM with fixed magnetic configuration contacts with a two-layer FM film. Twelve different types of magnetization curves $M(H)$ (both with and without hysteresis) have been found. Some of the $M(H)$ curves demonstrate unusual features, such as plateaus and inclined segments. The hysteresis loop becomes asymmetric if the surface anisotropy is taken into account.

PACS: 75.70.Cn Magnetic properties of interfaces (multilayers, superlattices, heterostructures);
75.60.Ch Domain walls and domain structure;
75.60.Ej Magnetization curves, hysteresis, Barkhausen and related effects.

Keywords: exchange bias, magnetic multilayers, hysteresis.

Introduction

Layered ferro/antiferromagnet (FM/AFM) systems are important objects for the read/write heads of modern data storage devices. They demonstrate the exchange bias effect [1–3], which consists in the shift of the hysteresis loop from the $H = 0$ position: $\mathbf{M}(\mathbf{H}) \neq -\mathbf{M}(-\mathbf{H})$ after field cooling. At the same time, coercivity is increased greatly. In recent experiments [4,5] asymmetric hysteresis loops, inclined segments of the $\mathbf{M} = \mathbf{M}(\mathbf{H})$ curves, and the horizontal plateaus (steps) in the $M(H)$ curves were observed. This complicated behavior is not caused by the kinetics of the magnetization reversal (by the finite rate of the field change in the experiment) and it is apparently caused by certain nonuniform and noncolinear (canted) states of the magnetic layers. This correlates with the fact that all modern theories of the exchange bias phenomenon [6–10] involve nonuniform states (domain walls or incomplete domain walls) and/or interface roughness to explain many peculiar features of this phenomenon.

In our previous works [11,12] two simple theoretical models of the FM/AFM bilayer with exchange bias: "two-spin model" and the "continuous model" were proposed. In particular, the two-spin model is the simplest possible model which allows nonuniform magnetic states. Despite simplicity, it can explain qualitatively many features of the exchange bias phenomenon. All possible magnetic structures of the two-spin model were found in Ref. 11, however the detailed study of the hysteresis phenomenon was beyond the scope of the previous paper. The properties of the domain walls in bilayer FM/AFM system with imperfect interface and their connection with the exchange bies phenomenon was discussed in Ref. 13.

The goal of the present paper is to determine all possible types of the $M(H)$ curves (all shapes of the hysteresis loops and the magnetization reversal without hysteresis) which arise in the two-spin model. This paper is organized as follows. Chapter 1 defines the two-spin model. Chapter 2 examines the regions of stability of different collinear phases and presents the mechanism of the onset of hysteresis. Chapter 3 lists all types of the $M(H)$ curves and defines the corresponding regions on the plane of system's parameters. Chapter 4 examines the hysteresis in the two-spin model in yet more detail. Chapter 5 briefly examines the case of the anisotropy constants being different for two FM layers (which simulates surface anisotropy). It is followed by the conclusion.

1. Model

The present paper uses the two-spin model introduced in Ref. 11. Consider a FM/AFM bilayer consisting of a magnetic hard AFM subsystem, in which all magnetic moments are fixed and do not rotate during field reversal, and a FM subsystem consisting of two magnetic layers. (In Ref. 12 it was demonstrated that many features of field dependencies of magnetization in the two-layer model and continuous model of thin FM layer are the same after renormalization of the exchange interaction constants. On the other hand maybe the two-layer system represents the particular case for the problem. In any case this model can be used for the description of real two-layer films, which are studied experimentally.) The magnetic state is determined by the rotation angles φ_i of the magnetization vectors in the easy plane. In addition, a weak easy-axis anisotropy in this plane is taken into account. It is also assumed that the external magnetic field is directed along the easy axis. The magnetic state of the system is assumed to be uniform along the interface. The energy of the systems is

$$E = -J_0 \cos\varphi_1 - J \cos(\varphi_1 - \varphi_2) - \frac{\beta_1}{2}\cos^2\varphi_1 - \\ - \frac{\beta_2}{2}\cos^2\varphi_2 - H(\cos\varphi_1 + \cos\varphi_2), \quad (1)$$

where J_0 is the exchange interaction across the interface (FM–AFM exchange, assumed to be ferromagnetic), J is the exchange interaction between two FM layers, β_i are the anisotropy constants for the two FM layers, and H is the external magnetic field. Indices numbers 1, 2 correspond to the layer adjacent to the interface and the second FM layer (on the free boundary of the FM), respectively. The possible equilibrium states are given by the equations $\partial E/\partial\varphi_i = 0$, $i = 1, 2$, namely:

$$(H + J_0)\sin\varphi_1 + J\sin(\varphi_1 - \varphi_2) + \beta_1 \sin\varphi_1\cos\varphi_1 = 0, \quad (2)$$

$$H\sin\varphi_2 + J\sin(\varphi_2 - \varphi_1) + \beta_2 \sin\varphi_2\cos\varphi_2 = 0. \quad (3)$$

First we note that the collinear structures (↑↑ and ↓↓ phases, $\varphi_1 = \varphi_2 = 0, \pi$) with vectors $\mathbf{M}_i$ parallel to each other and parallel or antiparallel to the direction of the magnetic field, respectively, are solutions of Eqs. (2), (3). The solutions with antiparallel directions of the vectors $\mathbf{M}_i$ (↑↓ and ↓↑ phases) also exist. In Secs. 1–4 we consider the case of equal anisotropy constants for the two FM layers: $\beta_1 = \beta_2 = \beta$ (the case $\beta_1 \neq \beta_2$ is studied in Sec. 5). Upon certain conditions there also exists a canted (non-collinear) solution of Eqs. (2), (3), with $\varphi_i \neq 0, \pi$. This is the two-spin equivalent of the "incomplete domain wall" object discussed in the exchange bias literature. In the presence of anisotropy (even for $\beta_1 = \beta_2$) the canted solutions $\varphi_i = \varphi_i(H)$ cannot be found analytically. It is easy to show that the magnetization curve $M(H)$ for $\beta_1 = \beta_2$ is antisymmetric with respect to the exchange bias field $H = -J_0/2$. (The energy (1) is invariant under the transformation $\phi_i \to \pi - \phi_i$, $H \to -J_0 - H$.) Hysteresis loop possessing this symmetry is called "symmetric hysteresis loop" in the exchange bias literature, and the opposite is the "asymmetric hysteresis loop" (see Sec. 5).

2. The boundaries of the hysteresis loop

In our previous work [11] the transformation of the collinear ↑↑ phase ($\varphi_1 = \varphi_2 = 0$) to the canted phase was considered. This transition corresponds to the bifurcation of the solution $\varphi_1 = \varphi_2 = 0$. At the vicinity of the bifurcation point, there are canted solutions of Eqs. (2), (3) which are infinitesimally close to the collinear phase. In order to find this point, we linearize Eqs. (2), (3) with respect to the angles φ_i and look for the nonzero solutions of the linearized equations. This gives the bifurcation field

$$H_{\uparrow\uparrow} = \left(\sqrt{J_0^2 + 4J^2} - (J_0 + 2J)\right)/2 - \beta. \quad (4)$$

It is marked in Fig. 1 as the point (a).

In the absence of hysteresis (see below) the ↑↑ phase is stable for $H > H_{\uparrow\uparrow}$, while for $H < H_{\uparrow\uparrow}$ the canted phase is stable. When hysteresis is present, however (as shown in Fig. 1), $H_{\uparrow\uparrow}$ gives the lower boundary on the hysteresis loop, and the canted phase is stable even for $H > H_{\uparrow\uparrow}$.

The dynamical stability of any given structure (collinear or canted) is determined by the Hessian of the potential energy surface $E = E(\varphi_1, \varphi_2)$, i.e.

$$K = \frac{\partial^2 E}{\partial\varphi_1^2}\frac{\partial^2 E}{\partial\varphi_2^2} - \left(\frac{\partial^2 E}{\partial\varphi_1\partial\varphi_2}\right)^2. \quad (5)$$

The structure in question is stable for $K > 0$, which corresponds to the minimum of the potential energy. At the saddle point of the potential energy surface ($K = 0$) the structure loses stability. For the collinear ↑↑ phase

$$K = (H + \beta)(H + J_0 + \beta) + J(2H + J_0 + 2\beta), \quad (6)$$

and, comparing with Eq. (4), we obtain the expected result that it loses stability exactly at the bifurcation point.

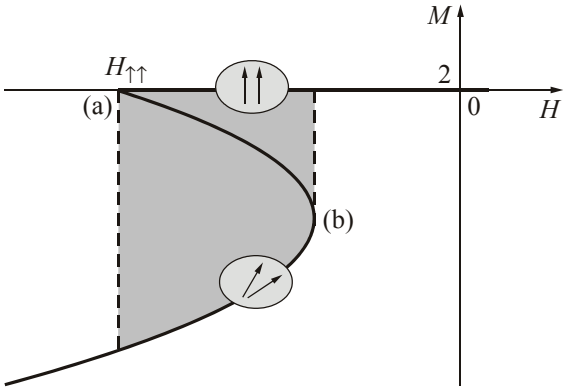

Fig. 1. The transformation of the collinear ↑↑ phase into the canted phase: (a) — bifurcation point, (b) — the point with $dM/dH = \infty$. The hysteresis loop is filled.

The analysis of the stability of the $\downarrow\downarrow$ phase ($\varphi_{1,2} = \pi$) can be done in a similar way, and the result is

$$H_{\downarrow\downarrow} = \left(-\sqrt{J_0^2 + 4J^2} + 2J - J_0\right)/2 + \beta\,. \qquad (7)$$

The antiparallel phase $\uparrow\downarrow$ ($\varphi_1 = 0,\ \varphi_2 = \pi$) corresponds to the plateau (a region with $M = \text{const}$, or, more specifically, $M = 0$ in this case) in the field dependence of magnetization $M(H)$. Another possible antiparallel phase, $\downarrow\uparrow$ ($\varphi_1 = \pi,\ \varphi_2 = 0$) always has higher energy compared to the $\uparrow\downarrow$ phase (for $J_0 > 0$), and therefore it is not important for the present paper. The antiparallel phases lose stability at

$$H_{\uparrow\downarrow} = -J_0/2 \pm \sqrt{(J_0/2 - J + \beta)^2 - J^2}\,. \qquad (8)$$

Equation (4) determines one of the boundaries of the hysteresis loop (or, in general, region of the magnetization reversal) in the H axis. As will be shown below, for small enough anisotropy there is no hysteresis and the magnetization switches via the uniform magnetization reversal process through a region of the canted phase. It roughly corresponds to the picture of both spins rotating as one with the change of H, with the angle $\varphi_1 - \varphi_2$ between two spins being rather small. The $\uparrow\uparrow$-canted phase transition is of the second order in this case.

The hysteresis appears when the derivative dM/dH for the canted phase becomes negative at the bifurcation point (see Fig. 1). To determine the critical values of the parameters for which the hysteresis appears ($dM/dH = \infty$), we find the slope of the $M(H)$ curve in the canted phase near the bifurcation point. To do this, we expand the Eqs. (2), (3) into the series with respect to the variables φ_i up to the cubic terms:

$$(H + J_0 + J + \beta)\varphi_1 - J\varphi_2 - \frac{1}{6}(H + J_0 + 4\beta)\varphi_1^3 - \\ - \frac{J}{6}(\varphi_1 - \varphi_2)^3 = 0\,, \qquad (9)$$

$$(H + J + \beta)\varphi_2 - J\varphi_1 - \frac{1}{6}(H + 4\beta)\varphi_2^3 + \frac{J}{6}(\varphi_1 - \varphi_2)^3 = 0\,, \qquad (10)$$

and look for the solutions in the form of power series with respect to the small deviations of the magnetic field from its bifurcation value $\varepsilon = \sqrt{H - H_{\uparrow\uparrow}}$: $\varphi_i \approx \varphi_i^{(0)}\varepsilon + \varphi_i^{(1)}\varepsilon^3 + \ldots$ In the first order in ε we obtain the bifurcation field and the relation between the amplitudes of the two angles:

$$\varphi_2 \approx \varphi_1(J_0 + J_1)/2J\,, \qquad (11)$$

where $J_1 = \sqrt{J_0^2 + 4J^2}$. In the third order in ε we obtain the values of the angles $\varphi_{1,2}$:

$$\varphi_{1,2}^2 \approx \frac{\varepsilon^2 J_1\,(J_1 \mp J_0)}{\beta(J_0^2 + 2J^2) - J^2(J_1 - 2J)}\,. \qquad (12)$$

The dependence of the magnetization of the system on the magnetic field near the bifurcation point is given by the formula

$$M(H) \approx 2 - (H - H_{\uparrow\uparrow})\frac{J_1^2}{\beta(J_0^2 + 2J^2) - J^2(J_1 - 2J)}\,. \qquad (13)$$

For the given values of the parameters J and J_0 the hysteresis appears for the critical value of the anisotropy parameter:

$$\beta_{c1} = J^2\,\frac{J_1 - 2J}{J_0^2 + 2J^2}\,. \qquad (14)$$

There is no hysteresis for $\beta < \beta_{c1}$. This is in a qualitative agreement with the experiment: for different systems with exchange bias both uniform magnetization reversal and hysteresis is observed.

3. Dependence of the shape of the hysteresis on the anisotropy parameter

In this section we analyze and classify all possible types of the $M(H)$ dependence (both with and without hysteresis) which arise in the model of Sec. 1 for different values of the anisotropy parameter β/J and the FM–AFM exchange parameter J_0/J. The numerical solution of the Eqs. (2), (3) was obtained by a relaxation algorithm. Namely, a (local) minimum of the total energy (1) is found by solving the system of differential equations $\partial\varphi_i/\partial t = -\partial E/\partial\varphi_i$ ($i = 1, 2$) numerically, which is done by the iterative procedure $\varphi_i \to \varphi_i - \varepsilon\,\partial E/\partial\varphi_i$, where ε is a sufficiently small parameter. The magnetization curves $M(H)$ corresponding to several characteristic values Z_i of the exchange interaction and anisotropy are depicted in Fig. 2. The points Z_i in the $(\beta/J,\ J_0/J)$ plane are presented in Fig. 3. In general there can be more than one local minimum of the energy $E(\varphi_i)$, which results in the hysteresis behavior. These minima can be found by starting the relaxation algorithm from different initial values of φ_i. To simulate the hysteresis, we ran the relaxation algorithm twice for each point Z_i and for each value of H, starting from the vicinity of the collinear phases $\uparrow\uparrow$ and $\downarrow\downarrow$, respectively (solid curves in Fig. 2). In addition, when appropriate, we started in the vicinity of the $\uparrow\downarrow$ phase, which sometimes gives new energy minima (dashed curves in Fig. 2).

In total, twelve different types of the $M(H)$ dependence were found. They correspond to the twelve different regions in the $(\beta/J,\ J_0/J)$ plane (Fig. 3). For each region, one point Z_i was chosen arbitrarily. The regions are separated by the curves $\beta_{ci}(J_0/J)$, $i = 1, \ldots, 5$ in Fig. 3. The expressions for $\beta_{c1} \ldots \beta_{c4}$ were found analytically (and verified by numerical simulations), while the curve $\beta_{c5}(J_0/J)$ was obtained numerically. Equation (14) gives the expression for the critical value β_{c1} of anisotropy for which the hysteresis appears. For $\beta < \beta_{c1}$ there is no hyste-

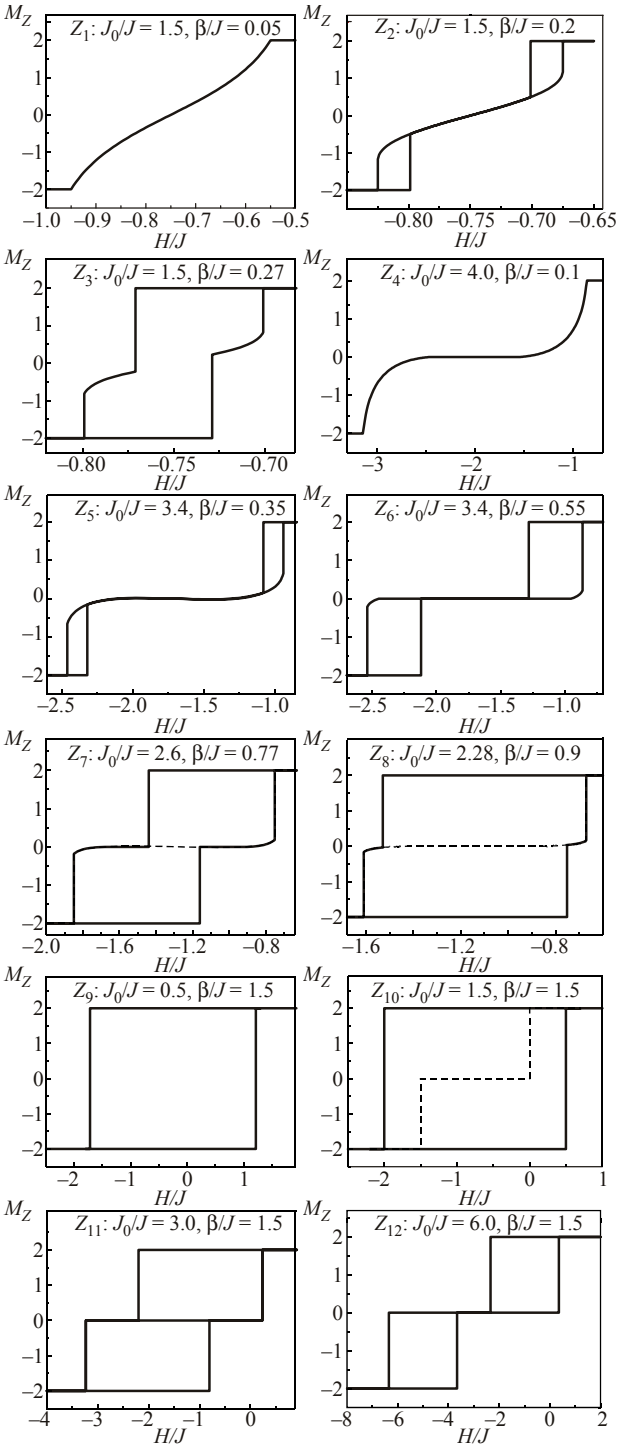

Fig. 2. Different shapes of the $M(H)$ hysteresis loop for different values of the magnetic anisotropy β/J and the FM–AFM exchange parameter J_0/J.

resis (Fig. 2, points Z_1, Z_4). The second critical value of anisotropy

$$\beta_{c2} = 1/2\left(\sqrt{4J^2 + J_0^2} - 2J\right)$$

is obtained from the condition $H_{\uparrow\uparrow} = H_{\downarrow\downarrow}$, where the expressions for $H_{\uparrow\uparrow}$, $H_{\downarrow\downarrow}$ are given by Eqs. (4), (7). For $\beta > \beta_{c2}$ there is a region of H for which both collinear phases (↑↑ and ↓↓) are dynamically stable. For

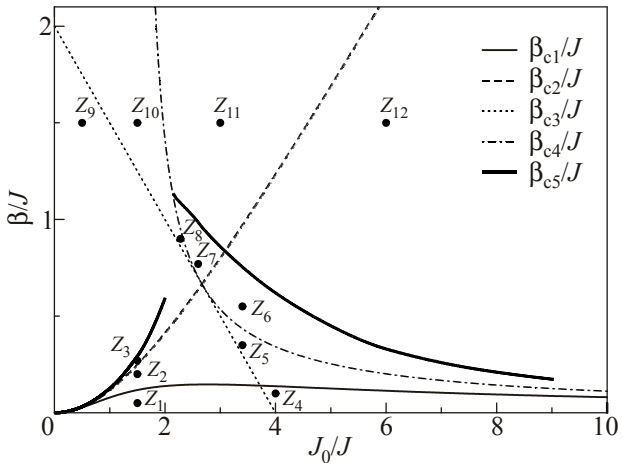

Fig. 3. Different types of the $M(H)$ dependence in the plane of the parameters (β / J, J_0/J).

$\beta_{c1} < \beta < \beta_{c2}$ there are two hysteresis loops separated by a region of the canted phase or ↑↓ phase (Fig. 2, points Z_2, Z_5, Z_6, Z_{12}). For $\beta > \beta_{c2}$, however, there is a single hysteresis loop (Fig. 2, points Z_3, $Z_7 - Z_{11}$). The third critical anisotropy β_{c3} correspond to the appearance of the $M = 0$ plateau (the ↑↓ phase). For $\beta > \beta_{c3}$ there is a $M = 0$ plateau in the $M(H)$ curve (Fig. 2, points $Z_5 - Z_8$, $Z_{10} - Z_{12}$). From the condition $H_{\uparrow\downarrow} = -J_0/2$, where $H_{\uparrow\downarrow}$ is given by Eq. (8), we obtain $\beta_{c3} = 2J - J_0/2$. The fourth critical anisotropy β_{c4} corresponds to the coexistence of the collinear phases ↑↑ (or ↓↓) and ↑↓. For $\beta_{c3} < \beta < \beta_{c4}$ the ↑↓ phase only appears in the middle of the region of the canted phase (Fig. 2, points Z_5, Z_8) or inside the hysteresis loop (Fig. 2, point Z_{10}). For $\beta > \beta_{c4}$ (Fig. 2, points Z_6, Z_7, Z_{11}, Z_{12}) the ↑↓ phase takes part in the formation of the hysteresis loop(s). The value of β_{c4} can be determined from the condition $H_{\uparrow\uparrow} = H_{\uparrow\downarrow}$, where $H_{\uparrow\downarrow}$ is given by the Eq. (8). It is given by the implicit expression

$$J_0 = \frac{\beta + J}{2\beta}\left(J + \sqrt{J^2 + 4\beta^2}\right) - \beta .$$

Finally, for $\beta > \beta_{c5}$ (Fig. 2, points Z_9–Z_{12}) the canted phase is suppressed and the hysteresis involves collinear phases only. Magnetization curves if Fig. 2 demonstrate experimentally observed [4,5] features, such as inclined segments and horizontal plateaus.

4. Regions of the hysteresis for the fixed values of the anisotropy

In this section we look at the hysteresis behavior in more detail. We fix the anisotropy β and the FM–AFM exchange J_0, and study the state of the system as the function of parameters J, H (Fig. 4). We rewrite the expressions (4), (7), (8) for the collinear-canted transition lines in the form $J = J(H, \beta, J_0)$:

$$J_1 = -\frac{(H+\beta)(H+J_0+\beta)}{(2H+J_0+2\beta)}, \quad (15)$$

$$J_3 = \frac{(H-\beta)(H+J_0-\beta)}{(2H+J_0-2\beta)}, \quad (16)$$

$$J_5 = -\frac{(H-\beta)(H+J_0+\beta)}{(J_0+2\beta)} \quad (17)$$

for the ↑↑ phase (line A_1 in Fig. 4), the ↓↓ phase (line A_3) and the ↑↓ phase (line A_5), respectively. Lines J_1, J_3 cross at the point $H = -J_0/2$, $J = J' = J_0^2/8\beta - \beta/2$. In the physical case of a small anisotropy $\beta \ll J_0$ near the crossing point we obtain $J \sim J_0^2/\beta \ll J_0$ and $J \approx J' - (J_0/\beta)^2 (H + J_0/2)/8$, respectively.

The upper boundary of the hysteresis loop corresponds to the value of H for which the derivative

$$dM/dH = -\sin\varphi_1 \; d\varphi_1/dH - \sin\varphi_2 \; d\varphi_2/dH$$

becomes infinite (point (b) in Fig. 1). It follows from the equations for $\varphi_i(H)$ (9), (10) that the derivatives $d\varphi_1/dH$ and $d\varphi_2/dH$ also become infinite at this H, which is given by

$$\left[\left(H+J_0\right)\cos\varphi_1 + 2\beta\cos^2\varphi_1 - \beta\right]\left(H\cos\varphi_2 + 2\beta\cos^2\varphi_2 - \beta\right) +$$
$$+\left[\left(H+J_0\right)\cos\varphi_1 + 2\beta\cos^2\varphi_1 + H\cos\varphi_2 + 2\beta\cos^2\varphi_2 - 2\beta\right] J\cos\left(\varphi_1 - \varphi_2\right) = 0, \quad (18)$$

where the angles φ_i are not know explicitly. The Eqs. (9), (10), (18) give the dependence $J_3 = J(H)$ for the right boundary of the hysteresis loop (see the line A_2 in Fig. 4). It follows from Eq. (18) that for the fixed anisotropy β there exists the maximum value of the exchange constant J for which the hysteresis takes place. It corresponds to $H = -J_0/2$ and

$$J = J'' = J_0^2\left(1 + \sqrt{1 + 32\beta^2/J_0^2}\right)/16\beta + \beta/2.$$

In the limit of a large enough exchange interaction $(J \sim 1/\beta)$ at the right boundary of hysteresis loop we obtain $\varphi_1 \approx \pi - \varphi_2 \approx \arccos(2\beta/J_0)$, $M \approx 8(\beta/J_0)^2$, and the right boundary of the hysteresis loop (line A_2 in Fig. 4) is given by $J \approx J'' - \left(J_0/\beta\right)\left(H + J_0/2\right)/4$.

The curves A_i in this figure determine the regions of existence of the different structures of the FM system and the hysteresis loops are located between the lines A_1A_2 and A_4A_3.

In Fig. 4 the domain of the stability of the parallel phase (↑↑) is situated to the right of the curve A_1, which starts at the point $H = -\beta$ in the limit $J \to 0$ and asymptotically approaches infinity as $H \to -J_0/2 - \beta$. The domain of the stability of the parallel phase (↓↓) is located on the left of the curve A_3, which starts at the point $H = -J_0 + \beta$ and asymptotically tends to the infinity as $H \to -J_0/2 + \beta$. The region below the curve A_5 (which lies between the points $H = -J_0 - \beta$ and $H = \beta$) corresponds to the antiparallel phase (↑↓). Finally, a triangular area between the curves A_1, A_3, A_5 corresponds to the canted phase. For the fixed anisotropy parameter, the shape of the hysteresis loop changes with the change of parameter J.

For the point Z_2 (see Fig. 4) the hysteresis loop splits into two loops (Fig. 2, Z_2). For the line A_5 (with

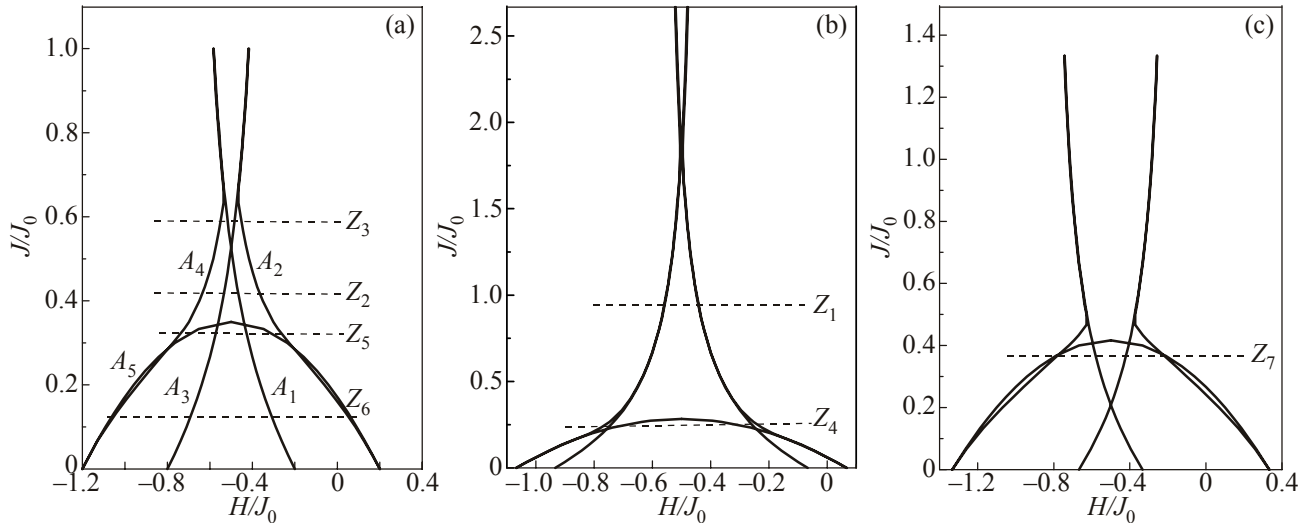

Fig. 4. Regions of the hysteresis in the plane of the parameters $(J/J_0, H/J_0)$ for the fixed values of the anisotropy β: $\beta/J_0 = 0.2$ (a), 0.066 (b), and 0.33 (c).

$J < J_0 + 2\beta$) we observe the plateau of the antiparallel phase ($\uparrow\downarrow$) in the $M(H)$ dependence (Fig. 2, Z_5). Upon further decrease of the exchange interaction, this plateau occupies the entire region between the hysteresis loops (Z_6), but the canted phase still remains inside each of the two hysteresis loops. If the magnetic anisotropy is small enough (Fig. 4(b)), there exists a domain of parameter J for which there is no hysteresis (in contrast to the FM systems without exchange bias).

5. The case of different anisotropy constants for the two FM layers ($\beta_1 \neq \beta_2$)

We now briefly consider the case $\beta_1 \neq \beta_2$, i.e., the case of different anisotropy constants for the two layers of the ferromagnet. This simulates the presence of the surface anisotropy arising due to the broken lattice symmetry at the FM/AFM interface. The Eqs. (4), (7), (8) for the boundary of the stability of various collinear phases change into

$$H_{\uparrow\uparrow} = -\frac{1}{2}(2J + J_0 + \beta_1 + \beta_2) + \frac{1}{2}\sqrt{4J^2 + (J_0 + \beta_1 - \beta_2)^2}\,, \quad (19)$$

$$H_{\downarrow\downarrow} = -\frac{1}{2}(-2J + J_0 - \beta_1 - \beta_2) - \frac{1}{2}\sqrt{4J^2 + (J_0 - \beta_1 + \beta_2)^2}\,, \quad (20)$$

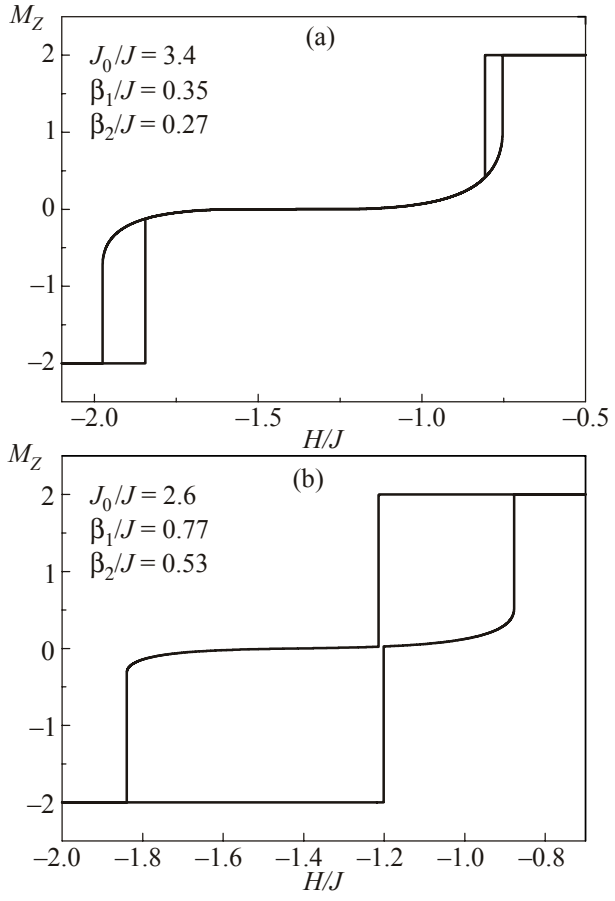

Fig. 5. Two typical magnetization curves $M(H)$ for the case $\beta_1 \neq \beta_2$.

$$H_{\uparrow\downarrow} = -\frac{1}{2}(J_0 + \beta_1 - \beta_2) + \frac{1}{2}\sqrt{(J_0 - \beta_1 - \beta_2)^2 + 2J_0(\beta_1 + \beta_2) + J_0^2 - 4JJ_0 - 4J^2}\,, \quad (21)$$

respectively. The number of different possible types of the $M(H)$ curves for this is extremely large. We do not attempt a complete classification here, instead in Fig. 5 we present two typical $M(H)$ curves with $\beta_1 \neq \beta_2$. One can easily see that the dependence $M(H)$ is no longer antisymmetric under transformation $H \to -J_0 - H$. In other words, for $\beta_1 \neq \beta_2$ asymmetric hysteresis loops are observed. This demonstrates on the qualitative level that the presence of surface anisotropy at the FM/AFM interface leads to an asymmetric hysteresis loop, an experimentally observed feature of the exchange bias systems.

Conclusion

In the present paper, we have studied both analytically and numerically the hysteresis phenomenon in a FM/AFM bilayer in the framework of the "two-spin model" (two layers of a ferromagnet in contact with a hard antiferromagnet). Twelve different types of the magnetization curves $M(H)$ (both with and without hysteresis) were found for different values of the parameters of the system (J_0/J and β/J). The explicit expressions for the boundaries of the respective regions of the (J_0/J, β/J) plane were obtained.

Also the case of different anisotropy constants for the two ferromagnetic layers (surface anisotropy) was considered. Asymmetric $M(H)$ curves were obtained in this case. Despite the simplicity of the model, it is able to reproduce many experimentally observed features of the exchange bias phenomenon.

Financial support Complex program NASU through the Grant "Fundamental problems of nanostructural systems, nanomaterials and nanotechnologies" is gratefully acknowledged.

1. W.H. Meiklejohn and C.P. Bean, *Phys. Rev.* **102**, 1413 (1956).
2. J. Nogues and I.K. Schuller, *J. Magn. Magn. Mater.* **192**, 203 (1999).
3. A.E. Berkowitz and K. Takano, *J. Magn. Magn. Mater.* **200**, 552 (1999).
4. D.N. Merenkov, A.N. Bludov, S.L. Gnatchenko, M. Baran, R. Szymchak, and V.A. Novosad, *Fiz. Nizk. Temp.* **33**, 1260 (2007) [*Low Temp Phys.* **33**, 957 (2007)].
5. S.L. Gnatchenko, D.N. Merenkov, A.N. Bludov, V.V. Pishko, Yu.A. Shakhaeva, M. Baran, R. Szymchak, and V.A. Novosad, *J. Magn. Magn. Mater*. **307**, 263 (2006).
6. M. Kiwi, *J. Magn. Mag. Mater* **234**, 584 (2001).
7. M.D. Stiles and R.D. McMichael, *Phys. Rev. B* **59**, 3722 (1999).

8. U. Nowak, K.D. Usadel, J. Keller, P. Miltényi, B. Beschoten, and G. Güntherodt, *Phys. Rev. B* **66**, 014430 (2002).
9. T.C. Schulthess and W.H. Butler, *Phys. Rev. Lett.* **81**, 4518 (1998).
10. Jing Chen, Guojun Jin, and Yu-qiang Ma, *J. Phys.: Condens. Matter* **19**, 236225 (2007).
11. A.G. Grechnev, A.C. Kovalev, and M.L. Pankratova, *Fiz. Nizk. Temp.* **35**, 670 (2009) [*Low Temp. Phys*. **35**, 526 (2009)].
12. A.G. Grechnev, A.C. Kovalev, and M.L. Pankratova, *Fiz. Nizk. Temp.* **35**, 603 (2009) [*Low Temp. Phys*. **35**, 476 (2009)].
13. A.S. Kovalev and M.L. Pankratova, *Fiz. Nizk. Temp.* **37**, 1085 (2011) [*Low Temp. Phys*. **37**, 866 (2011)].